Increased Frequency of Sediment Heatwaves in a Virginia Seagrass Meadow

Spencer J. Tassone[1,2*], Michael L. Pace[1]

[1]Department of Environmental Sciences, University of Virginia, Charlottesville, VA

[2]Department of Biological Sciences, Michigan Technological University, Houghton, MI

*Corresponding Author:

Spencer J. Tassone (ORCID iD: https://orcid.org/0000-0002-9340-7170)

Department of Biological Sciences

Michigan Technological University

740 Dow Building

Houghton, MI 49931

stassone@mtu.edu

Summary of Comments on Tassone_Pace_Sediment2023.pdf

Page: 1

Number: 1 Author: Reviewer Subject: Sticky Note Date: 12/19/2023 1:29:49 PM

Tassone, S.J., Pace, M.L. Increased Frequency of Sediment Heatwaves in a Virginia Seagrass Meadow. Estuaries and Coasts (2023). https://doi.org/10.1007/s12237-023-01314-7

Abstract

Coastal marine heatwaves have destructive and lasting impacts on foundational species and are increasing in frequency, duration, and magnitude. High atmospheric temperatures are often associated with marine heatwaves (MHW) which are defined as 5-days of water temperatures above a seasonally varying 90th percentile threshold. In this study we consider the prevalence of MHW propagation into surficial sediments to cause sediment heatwaves (SHW). Within a shallow, subtidal seagrass meadow in Virginia, USA, sediment temperature was measured at hourly intervals at a depth of 5 cm between June 2020-October 2022 at the meadow edge and central meadow interior. The observed sediment temperature, along with a 29-year record of water temperature and water level was used to develop a sediment temperature model for each location. Modeled sediment temperatures were used to identify sediment heatwaves that may thermally stress belowground seagrass. At both meadow locations, sediment heatwave frequency increased at a rate twice that of MHWs in the average global open ocean, coinciding with a 172% increase in the annual number of SHW days, from 11 to 30 days year^{-1} between 1994-2022. Sediment heatwaves at both meadow locations co-occurred with a MHW 79-81% of the time, with nearly all SHWs having a zero day lag. The top 10% most extreme MHWs and SHWs occurred between November and April when thermal stress to seagrass was unlikely. In June 2015 a SHW co-occurred with an anomalously long duration MHW that was associated with a 90% decline in seagrass from this system, suggesting that SHWs may have contributed to the observed seagrass loss. These results document heatwave propagation across the pelagic-sediment interface which likely occur broadly in shallow systems with impacts to critical coastal ecosystem processes and species dynamics.

Keywords

Disturbance, Heatwave, Seagrass, Sediment, Blue Carbon

Acknowledgements

We thank Patricia L. Wiberg, Karen J. McGlathery, and Julianne Quinn for helpful discussions and early revisions to this manuscript, and Jonathan A. Walter for assistance with the wavelet analysis. We thank the staff of the LTER-Virginia Coast Reserve (Cora Baird, Amelie Berger, Tom Burkett, Buck Doughty, Donna Fauber, Sophia Hoffman, David Lee, Jonah Morreale) for field assistance. This work was supported by funding from an NSF grant supporting the LTER-Virginia Coast Reserve (DEB 1832221) and the Jefferson Scholars Foundation.

Introduction

Extreme high temperature events are expected to continue increasing in frequency, magnitude, and duration in the atmosphere and the ocean (Meehl and Tebaldi 2004; Wuebbles et al. 2017; Frölicher et al. 2018; Oliver et al. 2018). In the marine environment, these discrete heatwaves, defined as local, seasonally varying prolonged periods (≥ 5 days) of anomalously warm (> 90^{th} percentile) water temperature, may disproportionately stress marine organisms and vegetated coastal ecosystems relative to longer-term increases in mean water temperature (Krumhansl et al. 2021; Serrano et al. 2021). Vegetated coastal ecosystems including, but not limited to, seagrass meadows, represent 5-8% of Earth's land surface, yet collectively store 20-30% of all soil carbon, often referred to as "blue" carbon for its location in oceanic sediments (hereafter, BC; Fourqurean et al. 2012; Nahlik and Fennessy 2016). While also being a major global carbon sink (Duarte et al. 2005; Fourqurean et al. 2012), vegetated coastal ecosystems provide other ecosystem services, including sediment stabilization, erosion protection, nutrient and pathogen filtration, and habitat supporting fisheries (Hansen and Reidenbach 2012; McGlathery et al. 2012; Lamb et al. 2017; Unsworth et al. 2018). These ecosystem services are impacted by marine heatwaves (MHW) that have been implicated in seagrass mass mortality (Collier and Waycott 2014; Berger et al. 2020; Strydom et al. 2020; Aoki et al. 2021), conversion of a seagrass meadow from autotrophy to heterotrophy (Berger et al. 2020), and BC loss from seagrass sediments (Arias-Ortiz et al. 2018; Aoki et al. 2021).

Marine heatwaves are generated by anomalous horizontal advective heat fluxes from currents and tides, vertical diffusive heat fluxes across the air-water interface, and larger-scale climate phenomena (Schlegel et al. 2017a; Holbrook et al. 2019). These extreme water temperature events are associated with atmospheric subsidence and high-pressure blocking, which enhances vertical heat fluxes by reducing cloud cover, wind speed, and relative humidity thereby increasing surface air temperature (Holbrook et al. 2019). Furthermore, reduced wind speed decreases oceanic upwelling intensity, thermocline depth, and turbulence, thereby promoting water column stability (Holbrook et al. 2019). Additionally, offshore MHW can be advected horizontally to coastal regions via anomalous ocean circulation patterns, which can be exacerbated by local circulation and geomorphic features (Schlegel et al. 2017a; Schlegel et al. 2017b).

In a recent survey of researchers, Macreadie et al. (2019) identified fundamental questions to advance BC science, including better characterization of disturbance events in sediments that impact long-term BC storage. While heatwaves are known to occur in the atmosphere (AHW) and the pelagic environment of vegetated coastal marine ecosystems (Wiberg 2023), there has been no study of heatwaves based on long-term data in vegetated coastal marine sediments. This is due to a lack of sediment temperature monitoring over many years as used in MHW analysis, difficulty in predicting when and where heatwaves will occur, and perception that sediment temperature is less variable than atmospheric and water temperature. Nonetheless, MHW events have doubled in duration in recent decades (Frölicher et al. 2018) and are increasing in frequency (Oliver et al. 2018), threatening above and below-ground BC storage, ecosystem resilience, and ecosystem services. Understanding MHW transfer into vegetated coastal sediments is, therefore, critical.

Shallow, subtidal seagrass meadows reduce current flow (Hansen and Reidenbach 2012) such that water temperature can become several degrees warmer in meadow interiors relative to meadow edges (Aoki et al. 2021; Berger 2021). This spatial heterogeneity in water temperature may at times exceed seagrass thermal stress thresholds within interior meadow regions. Such an event occurred in June 2015 when the restored *Zostera marina* seagrass meadow in South Bay, VA, experienced a 14-day MHW event associated with a 90% reduction in seagrass shoot density (Berger et al. 2020) and a 20% loss of buried BC (Aoki et al. 2021). The mass mortality of *Z. marina* was spatially heterogenous, with the interior meadow region experiencing the greatest loss. In contrast, the meadow's edge was undisturbed due in part to lower thermal stress provided by greater oceanic exchange from a nearby inlet (Berger 2021). However, it remains unclear if the decline in seagrass occurred, in part, due to prolonged extreme sediment temperature exposure.

To investigate discrete, yet prolonged extreme sediment temperatures, we measured sediment temperature at 5 cm depth within the interior and edge regions of the South Bay *Z. marina* meadow (locations separated by ~1.4 km) for 2.5 years. This record was used to model sediment temperature in relation to water temperature, water level, day of year, and hour. Using the long-term modeled sediment temperature, we quantified sediment heatwaves (SHWs) retroactively within the meadow to address the questions: 1) do heatwaves occur in vegetated coastal sediments? 2) if so, are there spatial differences and temporal trends in vegetated coastal SHW characteristics? and 3) specifically, did the MHW in June 2015 produce a concurrent SHW in South Bay? We hypothesized that MHWs would be transferred into shallow coastal sediments. However, whether and how frequently sediment temperatures exceed the 90th percentile for 5 consecutive days is unknown with the possibility that sediments buffer temperature extremes such that exceedances of the threshold are typically short-lived. As the water temperature at the edge of the South Bay seagrass meadow is cooler due to greater oceanic exchange with an inlet, we expected that the interior region of the meadow would experience a greater frequency, duration, and magnitude of SHWs relative to the edge. Lastly, due to the observed spatial heterogeneity in seagrass loss following the June 2015 MHW event, we hypothesized the meadow interior had a concurrent SHW while the edge did not.

Methods

Study Site

The region between the Virginia, USA mainland of the Delmarva peninsula and Virginia's 14 coastal barrier islands makes up the Virginia Coast Reserve (VCR). Immediately west of the barrier island Wreck Island is the shallow lagoon - South Bay, that has a mean depth of ≤ 1.5 m and tidal range = 1.2 m (Hansen and Reidenbach 2013; Safak et al. 2015). South Bay is bordered by oceanic inlets to the north and south of Wreck Island and by Man and Boy Channel toward the mainland to the west (specific latitudes and longitudes of the study are given below; Figure 1). *Z. marina* was locally extinct from the VCR system for ~70 years however, restoration seeding beginning in 1999 has led to a 20.3 km^2 continuous *Z. marina* meadow in South Bay (Orth et al. 2020). In June 2015, a 14-day MHW preceded a 90% reduction in *Z. marina* shoot density and a 20% reduction in stored BC within the central region of the South Bay meadow, which took 2-4 years to recover (Berger et al. 2020; Aoki et al. 2021).

Data Collection

We conducted continuous monitoring of sediment temperature at a depth of 5 cm between June 2020 and October 2022 at the central (37.2638 °N, 75.8153 °W) and northern edge (37.2773 °N, 75.8092 °W) of the South Bay seagrass meadow (~1.4 km apart). A depth of 5 cm was chosen from a visual inspection of where *Z. marina* rhizomes were most abundant. Sediment temperature was measured at one-hour intervals using new Onset HOBO pendant temperature data loggers with a factory temperature accuracy of ± 0.53 °C (accuracy < ± 0.53 °C between 0-40 °C; factory stated drift resolution < 0.1 °C $year^{-1}$). Within each location (i.e., central and edge), two data loggers were buried approximately 26 m apart in areas where seagrass shoot density was undisturbed (i.e., control sites) and areas where seagrass shoots were experimentally removed and allowed to recover (i.e., treatment sites; Tassone 2023). There was no difference in the sediment temperatures within each meadow location for undisturbed versus disturbed sites based on linear regression slopes and R^2 of 0.99 (SI Figure 1). We provide additional details on the experiment and treatment/control plots in the Supplement. The comparison of sediment temperature of the two types of plots indicated temperature was relatively consistent on the scale of at least tens of meters in this system. Therefore, sediment temperatures were averaged at each meadow location.

Water depth was measured continuously at 15-minute intervals between October-November 2021 using Onset HOBO Water Level Data Loggers. Over this time period, the meadow edge was, on average, 20 cm deeper (mean depth = 1.5 m) than the central location (1.2 m). Concurrent water temperature was measured within each location at a fixed height by zip-tying a temperature sensor sheathed in a 1.5-inch diameter steel tube to a vertical PVC pole 20 cm above the sediment surface to compare *in-situ* water temperature with *in-situ* sediment temperature. Water and sediment thermistors were replaced at monthly intervals between April-November and were deployed for the entirety of the winter months (December-March). Overall, sensor malfunction or loss resulted in 1.9% and 3.9% of the sediment temperature data being missing from the central and edge locations, respectively, while ≤ 0.7% of the water temperature data was missing from both locations. The observed sediment and water temperature data from South Bay are publically available via the Environmental Data Initative data portal (Tassone and Pace 2023).

Continuous meteorological and water temperature monitoring has been ongoing within the VCR since 1989 and 1994, respectively. Gap-filled daily mean atmospheric temperature collected from the VCR Oyster Meteorological Station (37.2909 °N, 75.9268 °W; Groleger et al. 2022), approximately 10 km west of South Bay, was used to determine long-term atmospheric temperature trends as well as characterize AHW for comparison with MHW. The National Oceanic and Atmospheric Administration's (NOAA) Wachapreague, VA tide station (station ID: 8631044; 37.6078 °N, 75.6858 °W) provides publicly-available, continuous hourly water temperature measurements. This NOAA monitoring station is approximately 38 km north of South Bay, and the water temperature record from this station was used to confirm the presence of the June 2015 MHW event (Aoki et al. 2021). Water temperature at this location is collected at a depth of 1.0 m below MLLW. Monitoring records from this station were accessed via the NOAA Tides & Currents webpage (tidesandcurrents.noaa.gov/stationhome.html?id=8631044). This station's water temperature time series was used to determine long-term water temperature trends and characterize MHWs in the VCR. Long-term monthly mean atmospheric and water temperature trend analyses were conducted using Seasonal-Kendall trend tests with Sen's slope estimates using the R package 'wql' (Jassby and Cloern 2017; Tassone et al. 2022a). Months with ≥ 10 missing days were removed prior to trend testing.

Model Development

The lack of long-term sediment temperature time series necessitated the development of sediment temperature models that used the continuous sediment temperature time series from each South Bay location as a dependent variable. Multiple-linear regression models of hourly sediment temperature for each South Bay meadow location were developed using Wachapreague water temperature and mean-centered water level (both spanning 1994-2022), day of the year (i.e., 1-365), and hour (i.e., 1-24) as covariates to account for diffusive, advective, seasonal, and diurnal temperature variability respectively. Using Wachapreague water temperature in our South Bay sediment temperature models was necessary as this was the only source of a long-term hourly water temperature record. This approach assumed that the difference in water temperature between Wachapreague and South Bay was negligible. This assumption was supported by the strong, positive linear relationships between concurrent hourly Wachapreague water temperature and water temperature at the South Bay edge (slope = 0.92, R^2 = 0.96) and central sites (slope = 0.96, R^2 = 0.97; SI Figure 2). Wachapreague time series gaps ≤ 5 hours were linearly interpolated prior to model development. Model building and validation used a 75:25 split-sample design, where 75% of the hourly observed sediment temperatures (n = 15,168) were randomly sampled and used as the dependent variable during model building. The remaining 25% of the hourly observed sediment temperatures (n = 5,056) were used to validate the model predictions. Model validation between the observed and predicted hourly sediment temperatures for each meadow location was assessed using linear regression. Wavelet transforms were used to detect the power spectrum in the water and sediment temperature time series at the central and edge locations using the R package 'biwavelet' (Gouhier et al. 2021).

Extreme Event Detection

Aquatic and sediment heatwave detection was determined using the conventional MHW definition such that a heatwave event occurs when the daily mean temperature exceeds a local, seasonally-varying 90th percentile threshold for ≥ 5 days and without a drop > 2 days below the threshold (Hobday et al. 2016). Atmospheric heatwaves used a similar definition as MHWs however, the threshold duration was ≥ 3 days, with no drop below the threshold during an event. The difference in these definitions is related to the increased temperature variability in the atmosphere relative to the water and convention within the atmospheric and oceanographic fields (Perkins and Alexander 2013; Oliver et al. 2021; Tassone et al. 2022b). The severity of all heatwaves was classified based on Hobday et al. (2018), which described heatwave event severity based upon multiples of the difference between the local climatology and the 90th

percentile threshold and the peak magnitude of the observed temperature. Heatwave event detection and classification were conducted using the R package 'heatwaveR' (Schlegel and Smit 2018). As heatwaves are rare events that can span monthly boundaries, long-term trends in heatwave metrics (i.e., frequency, duration, intensity) were conducted on annual time series using non-parametric Mann-Kendall tests with Sen's slope estimates ("Kendall" and "trend" R packages; McLeod 2011; Pohlert 2020; Tassone et al. 2022a). Influential data points within the non-parametric regressions were identified as those points with a Cook's distance (D_i) > 4/*n*, where *n* is the total number of observations. All statistical analyses were conducted in the R environment for statistical computing (R Core Team 2022) and are archived on GitHub (https://github.com/spencer-tassone/SedimentHeatwaves).

Results

Observed Sediment and Water Temperature

Sediment temperature at the central meadow and edge locations followed a northern hemisphere temperate seasonal cycle. The maximum summer (June-August of 2020-2022) sediment temperature of the central meadow (32.1 °C) was similar to the edge location (31.6 °C; Figure 2a). Both locations experienced similar low winter (December-February of 2021-2022) temperatures of 1.4 °C and 1.5 °C for the central meadow and edge, respectively. Daily mean sediment temperature at the central meadow was up to 4.1 °C greater than the edge during spring and summer (Figure 2b). Conversely, the daily mean sediment temperature at the edge was up to 1.1 °C greater than the central meadow during fall and winter.

Sediment temperature seasonality closely followed water temperature seasonality at both locations (SI Figure 3). The water temperature ranges were 2.6 °C and 2.3 °C greater than the sediment temperatures ranges at the central meadow and edge locations, respectively. Water temperature was generally warmer than sediment temperature during summer and cooler than the sediments during winter (Figure 3). The temperature difference range between the water and sediment was 8.6 °C and 6.0 °C at the edge and central locations, respectively. The water and sediment temperature power spectrum at the edge location had a diurnal (24-hour) and semi-diurnal (12-hour) periodicity, while the central sites had only a diurnal signal (SI Figure 4).

Modeled Sediment Temperature

All covariates (i.e., water temperature, mean-centered water level, day of the year, and hour) for the long-term multiple linear regression were statistically significant at the edge location (p-value < 0.001; Table 1). Similarly, all covariates were statistically significant for the central site, except for the mean-centered water level (p-value > 0.05; Table 1). There was an excellent fit between the validation data not used in the construction of the models and the predicted values from the models (Figure 4). The slope of the linear regression between the observed and predicted hourly sediment temperature for the central meadow was 0.98 ± 0.01 (± SE) and 0.97 ± 0.01 for the edge ($R^2 \geq 0.97$; Figure 4). Wachapreague water temperature and/or water level were missing for 2006, 2007, and 2017, limiting modeled sediment temperature availability for those periods (SI Figure 5).

Heatwaves

Between 1994-2022 there was a total of 125 AHWs in the VCR (Figure 5a). There was an average (± SD) of 4 ± 2 events year^{-1}, with a mean duration of 4 days and a maximum duration of 9 days (Table 2). The mean intensity of the AHWs was 2.1 °C above the seasonally adjusted 90th percentile threshold and was up to 15.7 °C above the threshold. AHWs occurred more in summer (35%), with the other seasons sharing between 21-22% of the remaining AHWs (Figure 6). All of the top 10% most intense AHW occurred between November-March, with 67% (n = 8) occurring in winter and the remaining 33% occurring in fall (n = 2) and spring (n = 2). Atmospheric heatwave frequency had a positive linear increase over the study period; however, this trend was not statistically significant (p-value > 0.05). Similarly, the annual total number of AHW days had a positive trend that was not statistically significant (Figure 5b). Cook's D_i values for the annual total number of AHW days were > $4/n$ in 1998 and 2014, suggestive of influential outliers in the regression model (D_i = 0.17 and 0.15 respectively). Additionally, there was a long-term air temperature trend with a slope of 0.032 °C year^{-1} (p-value < 0.001).

There were 67 MHWs during the 29-year study period, averaging 3 ± 2 events year^{-1} (Figure 5c). The mean MHW duration was 8 days and ranged up to 26 days (Table 2). The mean MHW intensity was 1.3 °C above the seasonally adjusted 90th percentile threshold and was up to 6.5 °C above the threshold. MHWs occurred most often in summer (34 %), followed by winter (25%), spring (24%), and fall (16%; Figure 6). The top 10% most intense MHWs occurred during winter (n = 4) and spring (n = 3) between December-April. Heatwave frequency in the water column significantly increased over the study duration at a rate of 0.09 events year^{-1} (p-value = 0.024; Figure 5c). The annual total number of MHW days significantly increased by 0.67 days year^{-1} (p-value = 0.022; Figure 5d), representing a 172% increase in the annual total number of heatwave days between 1994 (11 days) and 2022 (30 days). D_i exceeded $4/n$ for the annual total number of MHW days in 1995, 2020, and 2021 (D_i = 0.19, 0.35, 0.15 respectively). The 14-day duration of the June 2015 MHW event that impacted *Z. marina* in South Bay was in the 94th percentile of all Wachapreague MHW events between 1994-2022. Lastly, the long-term water temperature trend was 0.041 °C year^{-1} (p-value < 0.001).

Among the two SHW locations, there were 66 and 64 SHWs at the central and edge locations, respectively (Figure 5e, g). Annual SHW frequency was, on average, greater at the central meadow location (3 ± 2 events year^{-1}) relative to the meadow edge (2 ± 2 events year^{-1}; Table 2). The mean and maximum duration of SHWs were equal among locations, averaging 8 days and ranging up to a maximum duration of 25 days (Table 2). Similarly, the mean SHW intensity relative to the 90th percentile threshold was equal among locations (mean = 1.2 °C) however, the maximum intensity relative to the 90th percentile threshold was marginally greater at the central meadow location (max = 5.8 °C) relative to the edge location (max = 5.7 °C). Both central and edge locations had the greatest proportion of sediment heatwaves occur in summer (35% and 36%, respectively), followed by spring (26% and 27%, respectively), winter (23% and 20%, respectively), and fall (both 17%; Figure 6). The top 10% most intense SHWs occurred between November-April. Sediment heatwave frequency at both locations significantly increased at a rate of 0.10 events year^{-1} (p-values $\leq$ 0.015; Figure 5e, g). The annual total number of SHW days significantly increased at an equal rate of 0.67 days year^{-1} for each location, representing an increase from an average of 11 SHW days in 1994 to 30 SHW days in 2022 (p-values $\leq$ 0.041; Figure 5f, h). Cook's distance was > $4/n$ at the central sites in 2020 (D_i = 0.45) and at the edge sites in 1995 (D_i = 0.14) and 2020 (D_i = 0.47).

Of the 67 MHW events, 33% started during an active AHW event. Of those 22 co-occurring AHW and MHW events, the MHW lagged the AHW on average by 1 ± 1 day, with a maximum lag of 4 days. Sediment heatwaves co-occurred with an active MHW 79% of the time at the edge and 81% of the time at the central meadow location. Furthermore, the average lag time between MHWs and SHWs was zero days at both locations, and up to 1 day at the central meadow location. The 14-day MHW in June 2015 associated with the observed aboveground seagrass dieback co-occurred with a SHW at both locations (Figure 7). There was no lag between the June 2015 MHW and SHWs, with each persisting for 14 days (June 12, 2015 – June 25, 2015). Additionally, there were three atmospheric heat spikes (i.e., daily mean temperature > 90th percentile threshold for a duration < 3 days) and a single 3-day AHW (June 21-23, 2015) that occurred during the MHW and SHWs (Figure 7).

Discussion

The results answer our three original questions about 1) SHW occurrence, 2) SHW spatial patterns and temporal trends, and 3) whether the June 2015 MHW produced a concurrent SHW. First, SHWs were documented based on the modeled sediment temperature dynamics over a 29-year period. SHWs were similar at the central and edge locations and increased over the time period. Finally, there was a concurrent SHW at both sites during the 2015 MHW. MHWs were generally incorporated into shallow coastal sediments as 79-81% of the observed SHWs co-occurred with an active MHW. All but one of the SHWs that coincided with a MHW had a zero-day lag, suggesting that extreme water and sediment temperatures are in phase and strongly coupled.

MHWs in the VCR and SHWs in South Bay are increasing in frequency and annual total number of heatwave days between 1994-2022. There was a low number of annual MHWs and SHWs at the beginning of the record (1994-1997) and a high number of MHWs and SHWs at the end of the record (2019-2022) accounting for the the positive trend in MHWs and SHWs over time. For the water column, the linear rate of MHW frequency increase (0.09 events year^{-1}) was 2x greater than the open ocean global average of 0.045 events year^{-1} (Oliver et al. 2018). This increase in MHW frequency was accompanied by a 172% increase in the annual total MHW days from 11 in 1994 to 30 in 2022. The increase in the annual number of MHW days was less than the globally averaged open ocean (Oliver et al. 2018) yet in agreement with the coastal ocean region of the temperate north-Atlantic (Lima and Wethey 2012; Thoral et al. 2022). MHWs in the VCR are anticipated to increase in the future based on a recent model projection (Wiberg 2023).

For the sediments, the linear rate of SHW frequency increase at both locations was 0.1 events $year^{-1}$, which is marginally greater than the increasing rate of MHW frequency in the VCR. This greater rate of SHW frequency increase than MHW and ~20% non-synchronous SHW with MHW suggest an additional sediment heating mechanism or that MHWs at the NOAA Wachapreague tidal station differ somewhat from those in South Bay (~38 km southeast of the NOAA tidal station). The lack of long-term (> 20 years) continuous water temperature records from South Bay limits the ability to test for spatial differences in MHWs. Nonetheless, the annual rate of total SHW days at both locations matched MHWs, increasing from 11 to 30 days $year^{-1}$ during the study period.

The central meadow and edge locations had commensurate increasing rates of SHW frequency, annual total SHW days, the proportion of co-occurrence with MHWs, and SHW characteristics. These results did not support the hypothesis that SHW metrics would be greater at the central meadow relative to the edge due to greater oceanic exchange that reduces heating at the edge. Evidence of greater oceanic exchange at the meadow edge was observed as the pelagic and sediment temperature power spectrums exhibited semi-diurnal (12-hour) and diurnal (24-hour) periods, while the central location solely exhibited diurnal periods (SI Figure 3). Additionally, pelagic and sediment temperatures during the summer were often greater at the central location relative to the edge, but during winter, when the most extreme MHWs and SHWs occurred, the meadow edge was typically warmer than the central meadow.

The high proportion of MHW and SHW co-occurrence suggests that horizontal advective heat fluxes (transport of heat via tides and currents) within the South Bay lagoon drive SHWs in this system. The relatively low co-occurrence of AHW and MHW in South Bay (33%) further supports that horizontal rather than vertical heat flux (direct atmospheric heating of water and sediment) is the dominant driver of SHWs in this shallow coastal system. Coastal MHWs are driven, in part, by broad-scale processes such as anomalous oceanic and atmospheric circulation patterns, as well as local-scale influences such as circulation and bathymetric features (Schlegel et al. 2017a; Schlegel et al. 2017b). Moreover, the seagrass meadow we studied is shallow with a depth of < 0.25 m during some neap tides, therefore direct heating of the sediments from the atmosphere is possible. Overall, these features all affect temperature dynamics in the nearshore environment, with potential to cause heterogenous heat accumulation in some shallow locations promoting the possibility of MHWs especially with climate warming (Wiberg 2023). While attribution of MHWs was outside the scope of the present study, MHWs in South Bay can occur without an adjacent coastal ocean MHW (Aoki et al. 2021). Additionally, seagrass is known to alter circulation patterns in South Bay (Hansen and Reidenbach 2012) however, the presence of MHWs after seasonal seagrass senescence suggests additional features may promote localized MHW development.

Aboveground seagrass biomass loss from the central South Bay meadow region contrasted against the undisturbed seagrass at the meadow edge following the 14-day MHW in June 2015 suggested that the central meadow area had a concurrent SHW while the edge did not. This hypothesis was partially supported as a SHW at the central location started and ended on the same day as the June 2015 MHW. However, a concurrent SHW at the meadow edge also co-occurred with the June 2015 MHW. Differences in observed seagrass loss may be due, in part, to spatial differences in absolute sediment temperature between the meadow edge and interior, spatial differences in sediment organic matter (Oreska et al. 2017), hydrogen sulfide (H_2S) production (Berger 2021), and the extened duration of the MHW event. While *Z. marina* become thermally stressed at 28.6 °C (Berger 2021), heatwave metrics (i.e., climatology, 90th percentile threshold) are localized in space and their thresholds vary throughout the year. Having species specific knowledge of an organism's thermal stress threshold becomes important when linking MHWs to species-level impacts, particularly when the thermal stress threshold is exceeded for multiple days. While thermal stress thresholds are common for the aboveground portion of vegetation, much less is known about thermal stress related to the belowground portions of these organisms. The SHW in June 2015 at the central meadow location exceeded 28.6 °C for three consecutive days while the SHW at the meadow edge did not exceed the *Z. marina* thermal stress threshold. Additionally, high sediment temperatures are associated with increased H_2S production in marine sediments and increased sulfide isotope concentration in seagrass tissues (Berger 2021), which have sub-lethal and lethal impacts on *Z. marina* (Goodman et al. 1995; Pedersen et al. 2004; Höffle et al. 2011; Dooley et al. 2013). Furthermore, H_2S can become concentrated in marine sediments during organic matter decomposition (Dooley et al. 2013) and the fraction of organic matter in South Bay seagrass meadow sediments is up to 3x greater within the central meadow relative to the edge (Oreska et al. 2017). Lastly, while the intensity of the June 2015 MHW was moderate, the 14-day duration of the event was extreme, putting it in the 94th percentile of all MHWs observed during the study period. Strydom et al. (2020) modeled seagrass loss from a world heritage area following a MHW event and found MHW duration to be a significant predictor of seagrass loss. The duration of the MHW, increased H_2S production in the meadow interior, and presence of a co-occurring SHW that exceeded the *Z. marina* thermal stress threshold at the meadow interior but not the meadow edge likely contributed to the spatial differences in observed *Z. marina* loss (Aoki et al. 2021) following the June 2015 MHW.

Anomalously high sediment temperature events likely have ecosystem and species-level consequences. Optimal microbial temperatures during winter, when SHWs are most intense, are often 20 °C greater than ambient temperatures (Joint and Smale 2017) such that a SHW in winter could increase ecosystem respiration while primary production remains low due to light-limitation and seasonal phenology of marine plants. Additionally, summer SHW may enhance sediment respiration rates above primary production if the primary producers become thermally stressed. The enhancement of winter and summer ecosystem respiration might reduce sediment BC stocks, potentially impacting the ability of seagrass to sequester carbon and reducing the valuation of seagrass in carbon markets (Oreska et al. 2020). At a species level, surficial sediments in subtidal seagrass meadows do not typically provide thermal refugia for sessile and slow-moving organisms during MHWs, given the high proportion of MHW-SHW co-occurrence. This coupling could negatively impact ectothermic benthic marine organisms such as bivalves, foraminifera, and polychaetes which significantly contribute to bioturbation and biogeochemical cycling (Ouellette et al. 2004; Deldicq et al. 2021; Román et al. 2023). Additionally, the intensity of short-term MHWs can have contrasting impacts on the biogeochemical processes of benthic macrofaunal communities such that nutrient cycling rates are enhanced during moderate MHWs and depressed during strong MHWs (Kauppi and Villnäs 2022). Nonetheless, some organisms, including blue crabs (*Callinectes sapidus*), may benefit from increasing SHWs, particularly in the winter, as elevated bottom water temperatures are predicted to increase overwinter survival (Glandon et al. 2019).

Future studies should consider the vertical profile of SHWs to better understand the depth to which heatwaves propagate and how SHWs impact critical ecosystem processes, including BC storage, and biogeochemical cycling, as well as temperature-dependent processes such as ecosystem metabolism and species distributions. Moreover, subsequent studies should consider the role of sediment temperature in un-vegetated systems and where there may be a greater decoupling between water and sediment temperature, such as in deep meadows, systems with high turnover, or greater canopy heights.

Sediment heatwaves at a depth of 5 cm regularly co-occur with MHW events in the shallow, subtidal vegetated coastal sediments of South Bay, VA. Furthermore, MHWs and SHWs significantly increased in frequency as did the annual total number of heatwave days during the 29 years between 1994-2022. While there were differences in pelagic and sediment temperature periodicity, there were no substantial differences in SHW metrics between the central and edge meadow locations. The June 2015 MHW associated with the 90% decline in aboveground seagrass density, 20% loss in BC stocks, and metabolic conversion of the meadow from autotrophy to heterotrophy (Berger et al. 2020, Aoki et al. 2021) coincided with SHWs at the central and edge meadow locations which may have contributed to observed patterns in seagrass loss.

Overall, these results document SHWs in vegetated coastal sediments and indicate these events likely occur in a variety of aquatic systems. While our sediment temperature model did not account for how seagrass metrics (i.e., differences in canopy height, density, biomass) may impact sediment temperature, future studies should consider how these factors impact sediment temperature dynamics. Inclusion of seagrass metrics might improve the accuracy of our sediment temperature model, particularly between the years 1999-2007 when South Bay was actively undergoing a state change due to restoration efforts. Lastly, our study highlights the value of long-term monitoring programs, such as NOAA's Center for Operational Oceanographic Products and Services (CO-OPS) and NSF's Long-Term Ecological Research (LTER) program, to characterize emergent climate change signals such as coastal marine and sediment heatwaves.

References

Aoki, L. R., McGlathery, K. J., Wiberg, P. L., Oreska, M. P. J., Berger, A. C., Berg, P., & Orth, R. J. 2021. Seagrass Recovery Following Marine Heat Wave Influences Sediment Carbon Stocks. *Frontiers in Marine Science*, *7*, 576784. https://doi.org/10.3389/fmars.2020.576784

Arias-Ortiz, A., Serrano, O., Masqué, P., Lavery, P. S., Mueller, U., Kendrick, G. A., Rozaimi, M., Esteban, A., Fourqurean, J. W., Marbà, N., Mateo, M. A., Murray, K., Rule, M. J., & Duarte, C. M. 2018. A marine heatwave drives massive losses from the world's largest seagrass carbon stocks. *Nature Climate Change*, *8*(4), 338–344. https://doi.org/10.1038/s41558-018-0096-y

Berger , A. C. 2021. Long-term aquatic eddy-covariance measurements of seagrass meatabolism and ecosystem response to warming ocean. *University of Virginia, Environmental Sciences - Graduate School of Arts and Sciences*, Ph.D. Dissertation. https://doi.org/10.18130/wfh0-1f94

Berger, A. C., Berg, P., McGlathery, K. J., & Delgard, M. L. 2020. Long-term trends and resilience of seagrass metabolism: A decadal aquatic eddy covariance study. *Limnology and Oceanography*, 65(7), 1423–1438. https://doi.org/10.1002/lno.11397

Collier, C. J., & Waycott, M. 2014. Temperature extremes reduce seagrass growth and induce mortality. *Marine Pollution Bulletin*, 83(2), 483-490.

Deldicq, N., Langlet, D., Delaeter, C., Beaugrand, G., Seuront, L., & Bouchet, V. M. 2021. Effects of temperature on the behavior and metabolism of an intertidal foraminifera and consequences for benthic ecosystem functioning. *Scientific Reports*, 11(1), 4013.

Dooley, F. D., Wyllie-Echeverria, S., Roth, M. B., & Ward, P. D. 2013. Tolerance and response of Zostera marina seedlings to hydrogen sulfide. *Aquatic Botany*, 105, 7-10.

Duarte, C. M., Middelburg, J. J., & Caraco, N. 2005. Major role of marine vegetation on the oceanic carbon cycle. *Biogeosciences*, 2(1), 1-8.

Fourqurean, J. W., Duarte, C. M., Kennedy, H., Marbà, N., Holmer, M., Mateo, M. A., Apostolaki, E. T., Kendrick, G. A., Krause-Jensen, D., McGlathery, K. J., & Serrano, O. 2012. Seagrass ecosystems as a globally significant carbon stock. *Nature Geoscience*, 5(7), 505–509. https://doi.org/10.1038/ngeo1477

Frölicher, T. L., E. M. Fischer, and N. Gruber. 2018. Marine heatwaves under global warming. *Nature,* 560(7718): 360–364.

Glandon, H. L., Kilbourne, K. H., & Miller, T. J. 2019. Winter is (not) coming: Warming temperatures will affect the overwinter behavior and survival of blue crab. *PLOS ONE*, 14(7), e0219555.

Goodman, J. L., Moore, K. A., & Dennison, W. C. 1995. Photosynthetic responses of eelgrass

(*Zostera marina* L.) to light and sediment sulfide in a shallow barrier island lagoon. *Aquatic Botany*, 50(1), 37-47.

Gouhier, T. C., Grinsted, A., and Simko, V. 2021. R package {biwavelet}: Conduct univariate and bivariate wavelet analyses (Version 0.20.21). https://github.com/tgouhier/biwavelet

Groleger, N., Morreale, J., and Porter, J. H. 2022. Gap-filled Meteorological Data for the Virginia Coast Reserve LTER - 1989-2022. Virginia Coast Reserve Long-Term Ecological Research Project Data Publication knb-lter-vcr.337.2 https://doi.org/10.6073/pasta/4cf8f0db83783b71f7ee001d794e0016.

Hansen, J., & Reidenbach, M. 2012. Wave and tidally driven flows in eelgrass beds and their effect on sediment suspension. *Marine Ecology Progress Series*, 448, 271–287. https://doi.org/10.3354/meps09225

Hansen, J. C. R., & Reidenbach, M. A. 2013. Seasonal Growth and Senescence of a Zostera marina Seagrass Meadow Alters Wave-Dominated Flow and Sediment Suspension Within a Coastal Bay. *Estuaries and Coasts*, 36(6), 1099–1114. https://doi.org/10.1007/s12237-013-9620-5

Hobday, A. J., Alexander, L. V., Perkins, S. E., Smale, D. A., Straub, S. C., Oliver, E. C. J., Benthuysen, J. A., Burrows, M. T., Donat, M. G., Feng, M., Holbrook, N. J., Moore, P. J., Scannell, H. A., Sen Gupta, A., and Wernberg, T. 2016. A hierarchical approach to defining marine heatwaves. *Progress in Oceanography*, 141, 227–238. https://doi.org/10.1016/j.pocean.2015.12.014

Hobday, A., Oliver, E., Sen Gupta, A., Benthuysen, J., Burrows, M., Donat, M., Holbrook, N., Moore, P., Thomsen, M., Wernberg, T., and Smale, D. 2018. Categorizing and Naming Marine Heatwaves. *Oceanography*, 31(2). https://doi.org/10.5670/oceanog.2018.205

Höffle, H., Thomsen, M. S., & Holmer, M. 2011. High mortality of Zostera marina under high temperature regimes but minor effects of the invasive macroalgae Gracilaria vermiculophylla. *Estuarine, Coastal and Shelf Science*, 92(1), 35-46.

Holbrook, N.J., Scannell, H.A., Sen Gupta, A., Benthuysen, J.A., Feng, M., Oliver, E.C., Alexander, L.V., Burrows, M.T., Donat, M.G., Hobday, A.J. and Moore, P.J., 2019. A global assessment of marine heatwaves and their drivers. *Nature Communications*, 10(1), 1-13. https://doi.org/10.1038/s41467-019-10206-z

Jassby, A. D., and Cloern, J. E. 2017. wq: Some tools for exploring water quality monitoring data. R package version 0.4.9 https://cran.r-project.org/package=wq

Joint, I., & Smale, D. A. 2017. Marine heatwaves and optimal temperatures for microbial assemblage activity. *FEMS Microbiology Ecology*, 93(2), fiw243. https://doi.org/10.1093/femsec/fiw243

Krumhansl, K. A., Dowd, M., and Wong, M. C. 2021. Multiple metrics of temperature, light, and water motion drive gradients in eelgrass productivity and resilience. *Frontiers in Marine*

Science, 8:597707. https://doi.org/10.3389/fmars.2021.597707

Lamb, J. B., van de Water, J. A. J. M., Bourne, D. G., Altier, C., Hein, M. Y., Fiorenza, E. A., Abu, N., Jompa, J., & Harvell, C. D. 2017. Seagrass ecosystems reduce exposure to bacterial pathogens of humans, fishes, and invertebrates. *Science*, 355(6326), 731–733. https://doi.org/10.1126/science.aal1956

Lima, F. P., & Wethey, D. S. 2012. Three decades of high-resolution coastal sea surface temperatures reveal more than warming. *Nature Communications*, 3(1), 704. https://doi.org/10.1038/ncomms1713

Macreadie, P. I., Anton, A., Raven, J. A., Beaumont, N., Connolly, R. M., Friess, D. A., Kelleway, J. J., Kennedy, H., Kuwae, T., Lavery, P. S., Lovelock, C. E., Smale, D. A., Apostolaki, E. T., Atwood, T. B., Baldock, J., Bianchi, T. S., Chmura, G. L., Eyre, B. D., Fourqurean, J. W., … Duarte, C. M. 2019. The future of Blue Carbon science. *Nature Communications*, 10(1), 3998. https://doi.org/10.1038/s41467-019-11693-w

McGlathery, K., Reynolds, L., Cole, L., Orth, R., Marion, S., & Schwarzschild, A. 2012. Recovery trajectories during state change from bare sediment to eelgrass dominance. *Marine Ecology Progress Series*, 448, 209–221. https://doi.org/10.3354/meps09574

McLeod, A. I. 2011. Kendall: Kendall rank correlation and Mann-Kendall trend test. R package version 2.2. https://CRAN.R-project.org/package=Kendall

Meehl, G. A., & Tebaldi, C. 2004. More Intense, More Frequent, and Longer Lasting Heat Waves in the 21st Century. *Science*, 305(5686), 994–997. https://doi.org/10.1126/science.1098704

Nahlik, A. M., & Fennessy, M. S. 2016. Carbon storage in US wetlands. *Nature Communications*, 7(1), 1-9.

Oliver, E. C. J., Benthuysen, J. A., Darmaraki, S., Donat, M. G., Hobday, A. J., Holbrook, N. J., Schlegel, R. W., & Sen Gupta, A. 2021. Marine Heatwaves. *Annual Review of Marine Science*, 13(1), 313–342. https://doi.org/10.1146/annurev-marine-032720-095144

Oliver, E. C. J., Donat, M. G., Burrows, M. T., Moore, P. J., Smale, D. A., Alexander, L. V., Benthuysen, J. A., Feng, M., Sen Gupta, A., Hobday, A. J., Holbrook, N. J., Perkins-Kirkpatrick, S. E., Scannell, H. A., Straub, S. C., & Wernberg, T. 2018. Longer and more frequent marine heatwaves over the past century. *Nature Communications*, 9(1), 1324. https://doi.org/10.1038/s41467-018-03732-9

Oreska, M. P. J., McGlathery, K. J., Aoki, L. R., Berger, A. C., Berg, P., & Mullins, L. 2020. The greenhouse gas offset potential from seagrass restoration. *Scientific Reports*, 10(1), 7325. https://doi.org/10.1038/s41598-020-64094-1

Oreska, M. P. J., McGlathery, K. J., & Porter, J. H. 2017. Seagrass blue carbon spatial patterns at the meadow-scale. *PLOS ONE*, 12(4), e0176630. https://doi.org/10.1371/journal.pone.0176630

Orth, R. J., Lefcheck, J. S., McGlathery, K. S., Aoki, L., Luckenbach, M. W., Moore, K. A., Oreska, M. P. J., Snyder, R., Wilcox, D. J., & Lusk, B. 2020. Restoration of seagrass habitat leads to rapid recovery of coastal ecosystem services. *Science Advances*, 6(41), eabc6434. https://doi.org/10.1126/sciadv.abc6434

Ouellette, D., Desrosiers, G., Gagne, J. P., Gilbert, F., Poggiale, J. C., Blier, P. U., & Stora, G. 2004. Effects of temperature on in vitro sediment reworking processes by a gallery biodiffusor, the polychaete *Neanthes virens*. *Marine Ecology Progress Series*, 266, 185-193. https://doi.org/ 10.3354/meps266185

Pedersen, O., Binzer, T., & Borum, J. 2004. Sulphide intrusion in eelgrass (*Zostera marina* L.). *Plant, Cell and Environment*, 27(5), 595–602. https://doi.org/10.1111/j.1365-3040.2004.01173.x

Perkins, S. E., & Alexander, L. V. 2013. On the Measurement of Heat Waves. *Journal of Climate*, 26(13), 4500–4517. https://doi.org/10.1175/JCLI-D-12-00383.1

Pohlert, T. 2020. trend: Non-Parametric Trend Tests and Change-Point Detection. R package version 1.1.4. https://CRAN.R-project.org/package=trend

R Core Team. 2022. R: A language and environment for statistical computing. R Foundation for Statistical Computing, Vienna, Austria. https://www.R-project.org/.

Román, M., Gilbert, F., Viejo, R. M., Román, S., Troncoso, J. S., Vázquez, E., & Olabarria, C. 2023. Are clam-seagrass interactions affected by heatwaves during emersion? *Marine Environmental Research*, 186, 105906.

Safak, I., Wiberg, P. L., Richardson, D. L., & Kurum, M. O. 2015. Controls on residence time and exchange in a system of shallow coastal bays. *Continental Shelf Research*, 97, 7–20. https://doi.org/10.1016/j.csr.2015.01.009

Serrano, O., Arias-Ortiz, A., Duarte, C. M., Kendrick, G. A., Lavery, P.S. 2021. Impact of Marine Heatwaves on Seagrass Ecosystems. In: Canadell, J. G., Jackson, R. B. (eds) Ecosystem Collapse and Climate Change. Ecological Studies, vol 241. Springer, Cham. https://doi.org/10.1007/978-3-030-71330-0_13

Schlegel, R. W., Oliver, E. C. J., Perkins-Kirkpatrick, S., Kruger, A., & Smit, A. J. 2017a. Predominant Atmospheric and Oceanic Patterns during Coastal Marine Heatwaves. *Frontiers in Marine Science*, 4, 323. https://doi.org/10.3389/fmars.2017.00323

Schlegel, R. W., Oliver, E. C. J., Wernberg, T., & Smit, A. J. 2017b. Nearshore and offshore co-occurrence of marine heatwaves and cold-spells. *Progress in Oceanography*, 151, 189–205. https://doi.org/10.1016/j.pocean.2017.01.004

Schlegel, R. W., & J. Smit, A. 2018. heatwaveR: A central algorithm for the detection of heatwaves and cold-spells. *Journal of Open Source Software*, 3(27), 821. https://doi.org/10.21105/joss.00821

Strydom, S., Murray, K., Wilson, S., Huntley, B., Rule, M., Heithaus, M., Bessey, C., Kendrick, G. A., Burkholder, D., Fraser, M. W., & Zdunic, K. 2020. Too hot to handle: Unprecedented seagrass death driven by marine heatwave in a World Heritage Area. *Global Change Biology*, 26(6), 3525-3538. https://doi.org/10.1111/gcb.15065

Tassone , S. J. 2023. Quantifying heatwaves and seagrass recovery dynamics in aquatic ecosystems. *University of Virginia, Environmental Sciences - Graduate School of Arts and Sciences*, Ph.D. Dissertation. https://doi.org/10.18130/0vkc-jj16

Tassone, S. J., Besterman, A. F., Buelo, C. D., Ha, D. T., Walter, J. A., & Pace, M. L. 2022a. Increasing heatwave frequency in streams and rivers of the United States. *Limnology and Oceanography Letters*, lol2.10284. https://doi.org/10.1002/lol2.10284

Tassone, S. J., Besterman, A. F., Buelo, C. D., Walter, J. A., & Pace, M. L. 2022b. Co-occurrence of Aquatic Heatwaves with Atmospheric Heatwaves, Low Dissolved Oxygen, and Low pH Events in Estuarine Ecosystems. *Estuaries and Coasts*, 45(3), 707–720. https://doi.org/10.1007/s12237-021-01009-x

Tassone, S. and M.L. Pace. 2023. High-frequency water and sediment temperature from the Seagrass Recovery Experiment, South Bay, VA 2020-2022 ver 1. *Environmental Data Initiative*. https://doi.org/10.6073/pasta/9d0556bf46a3a79b6bde96003529f407

Thoral, F., Montie, S., Thomsen, M. S., Tait, L. W., Pinkerton, M. H., & Schiel, D. R. 2022. Unravelling seasonal trends in coastal marine heatwave metrics across global biogeographical realms. *Scientific Reports*, 12(1), 7740. https://doi.org/10.1038/s41598-022-11908-z

Unsworth, R. K. F., Collier, C. J., Waycott, M., Mckenzie, L. J., & Cullen-Unsworth, L. C. 2015. A framework for the resilience of seagrass ecosystems. *Marine Pollution Bulletin*, 100(1), 34–46. https://doi.org/10.1016/j.marpolbul.2015.08.016

Wiberg, P. L. 2023. Temperature amplification and marine heatwave alteration in shallow coastal bays. Frontiers in Marine Science 10: https://doi.org/10.3389/fmars.2023.1129295

Wuebbles, D. J., Fahey, D. W., Hibbard, K. A., DeAngelo, B., Doherty, S., Hayhoe, K., Horton, R., Kossin, J. P., Taylor, P. C., Waple, A. M., & Yohe, C. P. 2017. Executive summary. Climate Science Special Report: Fourth National Climate Assessment, Volume I. U.S. Global Change Research Program. https://doi.org/10.7930/J0DJ5CTG

Tables & Figures

Table 1. Multiple linear regression model characteristics for South Bay sediment temperature. The long-term mean was removed from the Water Level variable prior to model development.

Location	Variable	Estimate ± SE	Variable p-val.	Adj. R^2	Model p-val.
Edge	Intercept	0.782 ± 0.034	< 0.001	0.974	< 0.001
	Water Temp. (°C)	0.879 ± 0.001	< 0.001		
	Water Level (m)	-0.744 ± 0.053	< 0.001		
	Day of Year	0.005 ± 0	< 0.001		
	Hour	0.01 ± 0.002	< 0.001		
Central	Intercept	0.513 ± 0.029	< 0.001	0.982	< 0.001
	Water Temp. (°C)	0.934 ± 0.001	< 0.001		
	Water Level (m)	0.022 ± 0.045	0.623		
	Day of Year	0.003 ± 0	< 0.001		
	Hour	0.02 ± 0.001	< 0.001		

Table 2. Heatwave characteristics for the VCR atmosphere at Oyster, VA, water column of South Bay, VA, and the sediments at the edge and central South Bay meadow locations. Frequency results are the annual mean number of events ± standard deviation.

Variable	Atmosphere	Water	Edge	Central
Total Events	125	67	64	66
Frequency (events year $^{-1}$)	4 ± 2	3 ± 2	2 ± 2	3 ± 2
Mean Duration (days)	4	8	8	8
Max Duration (days)	9	26	25	25
Mean Intensity - Rel. Thres. (^{o}C)	2.1	1.3	1.2	1.2
Max Intensity - Rel. Thres. (^{o}C)	15.7	6.5	5.7	5.8

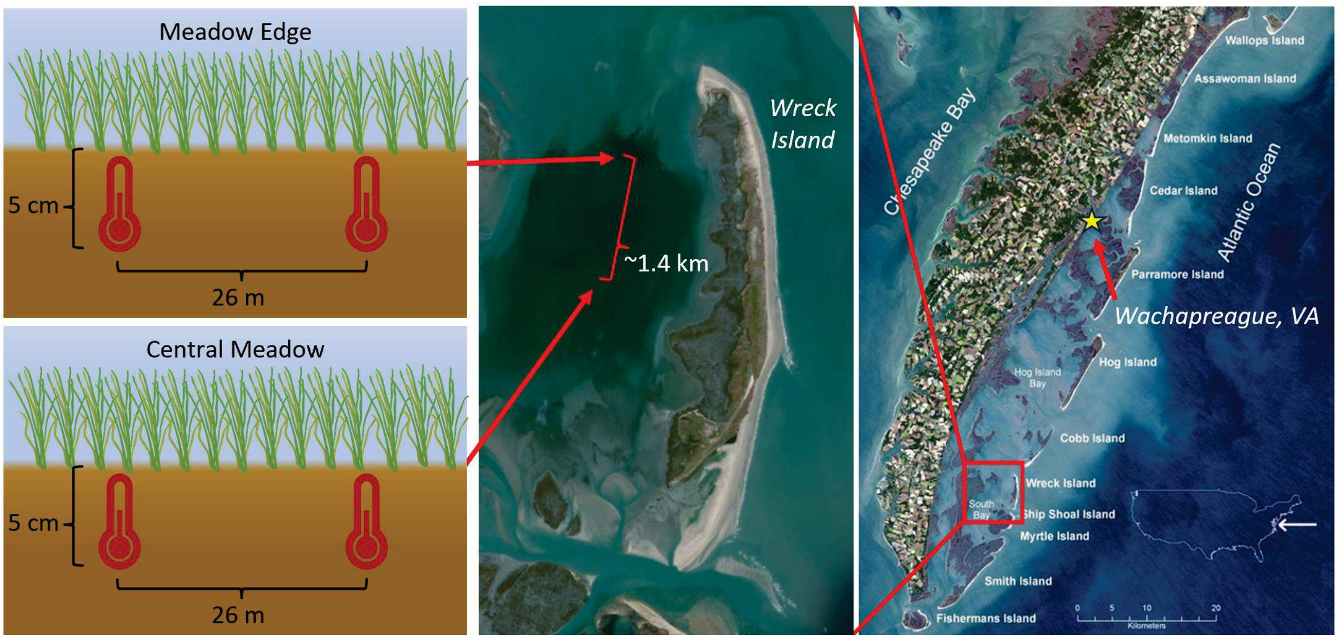

Figure 1. Map of the study area along with the position of sediment temperature thermistors (not to scale). Two temperature thermistors were buried to a depth of 5 cm at the meadow edge and central meadow interior which were approximately 1.4 km apart. Within each location, thermistors were spaced 26 meters apart. NOAA's tidal monitoring station at Wachapreague, VA, is denoted by a star in the right panel and is approximately 38 km north of South Bay.

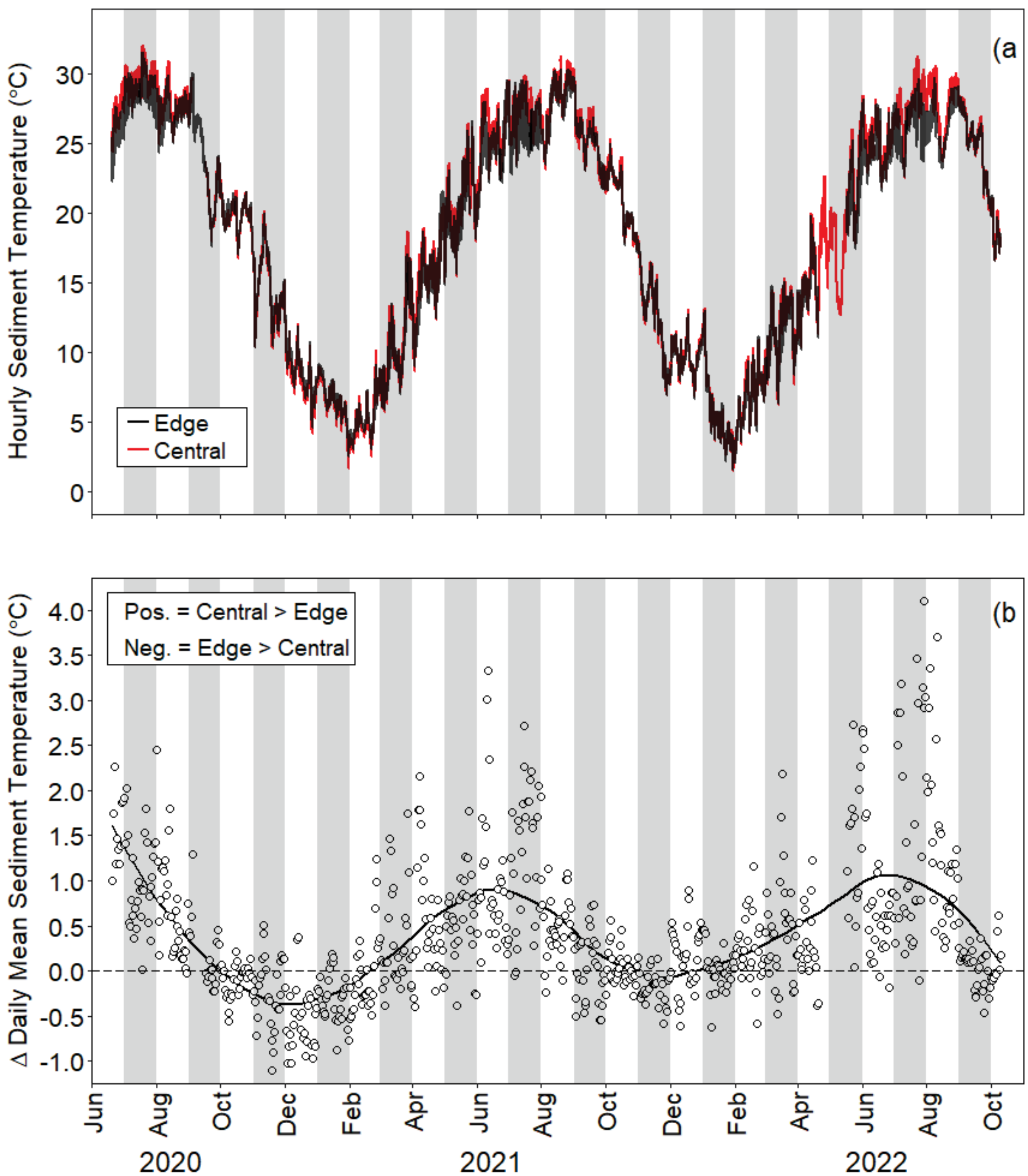

Figure 2. Hourly sediment temperature for the edge and central locations within the South Bay seagrass meadow (a). Daily mean difference in sediment temperature between the edge and central locations within South Bay (b). Positive values indicate that the central site was warmer than the edge, whereas negative values indicated that the edge was warmer than the central site. Dots represent the daily mean difference, while the smoothing line was produced using locally weighted polynomial regression.

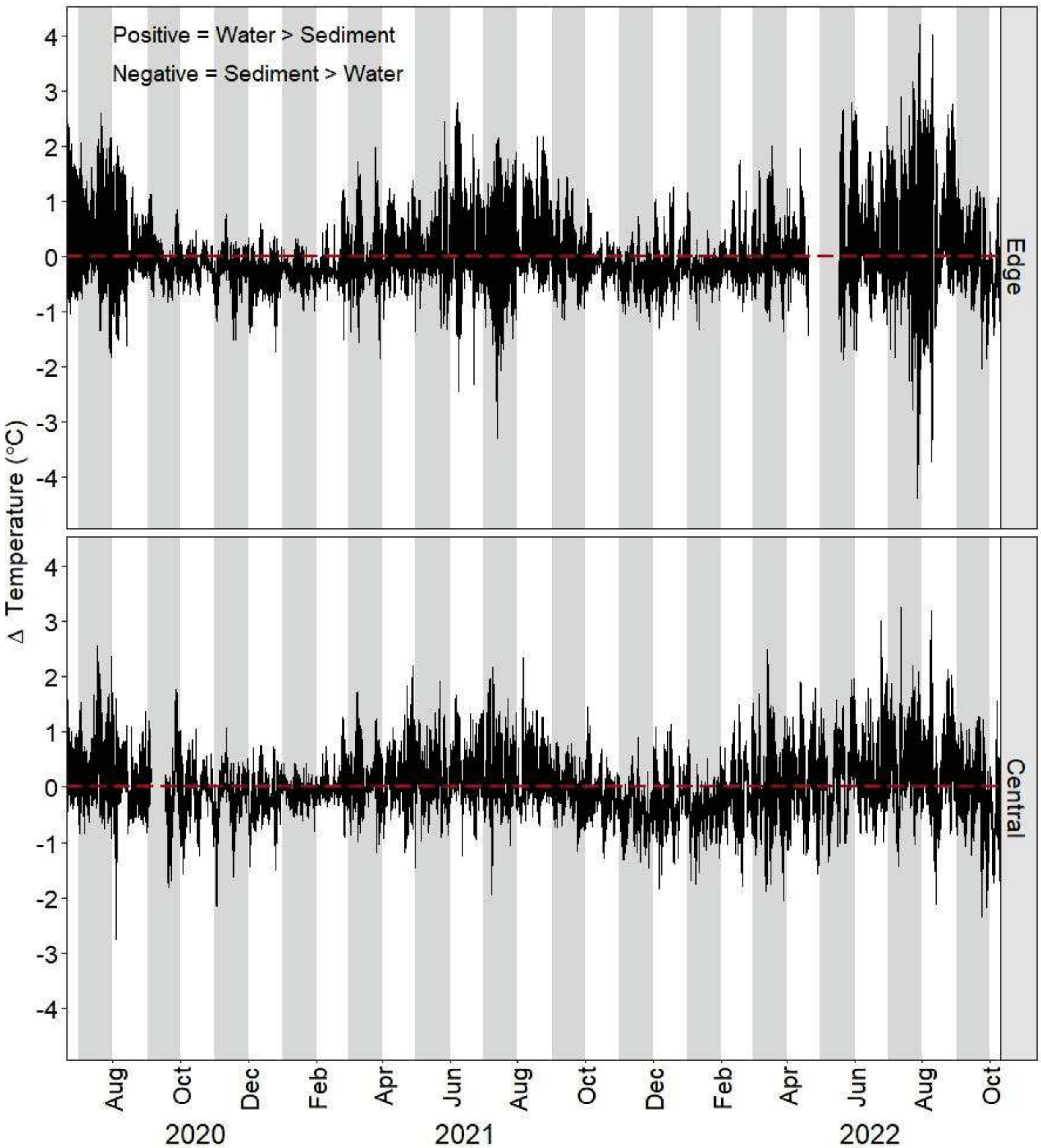

Figure 3. Observed hourly difference between water and sediment temperature for the edge and central locations. Positive values indicate that the water temperature was greater than the sediment temperature, whereas negative values indicate that the sediment temperature was greater than the water temperature.

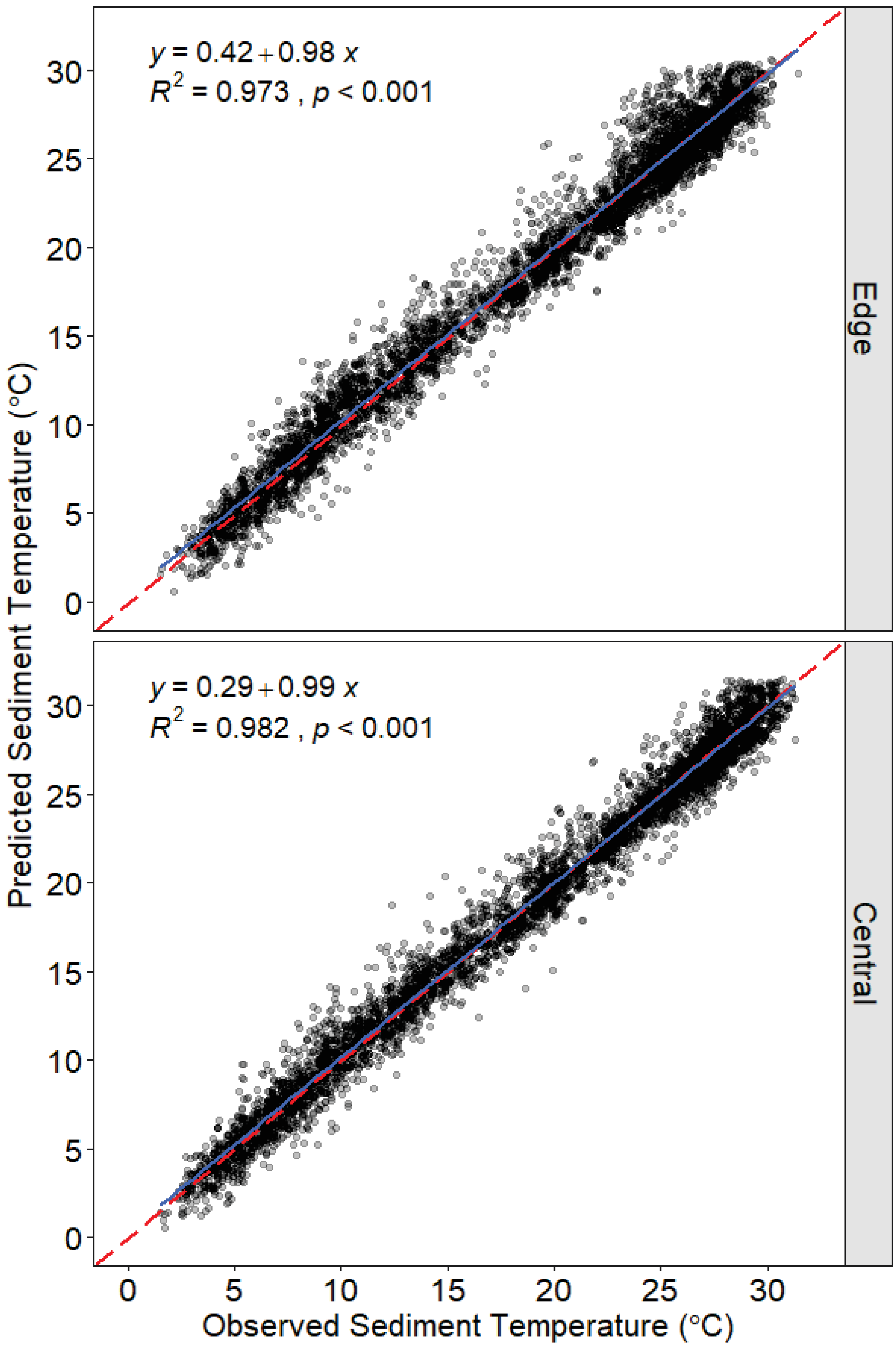

Figure 4. Sediment temperature model validation for the edge (top) and central meadow (bottom) locations of the South Bay seagrass meadow. The red dashed lines represent the 1:1 line, while the blue lines represent the line of best fit from linear regression.

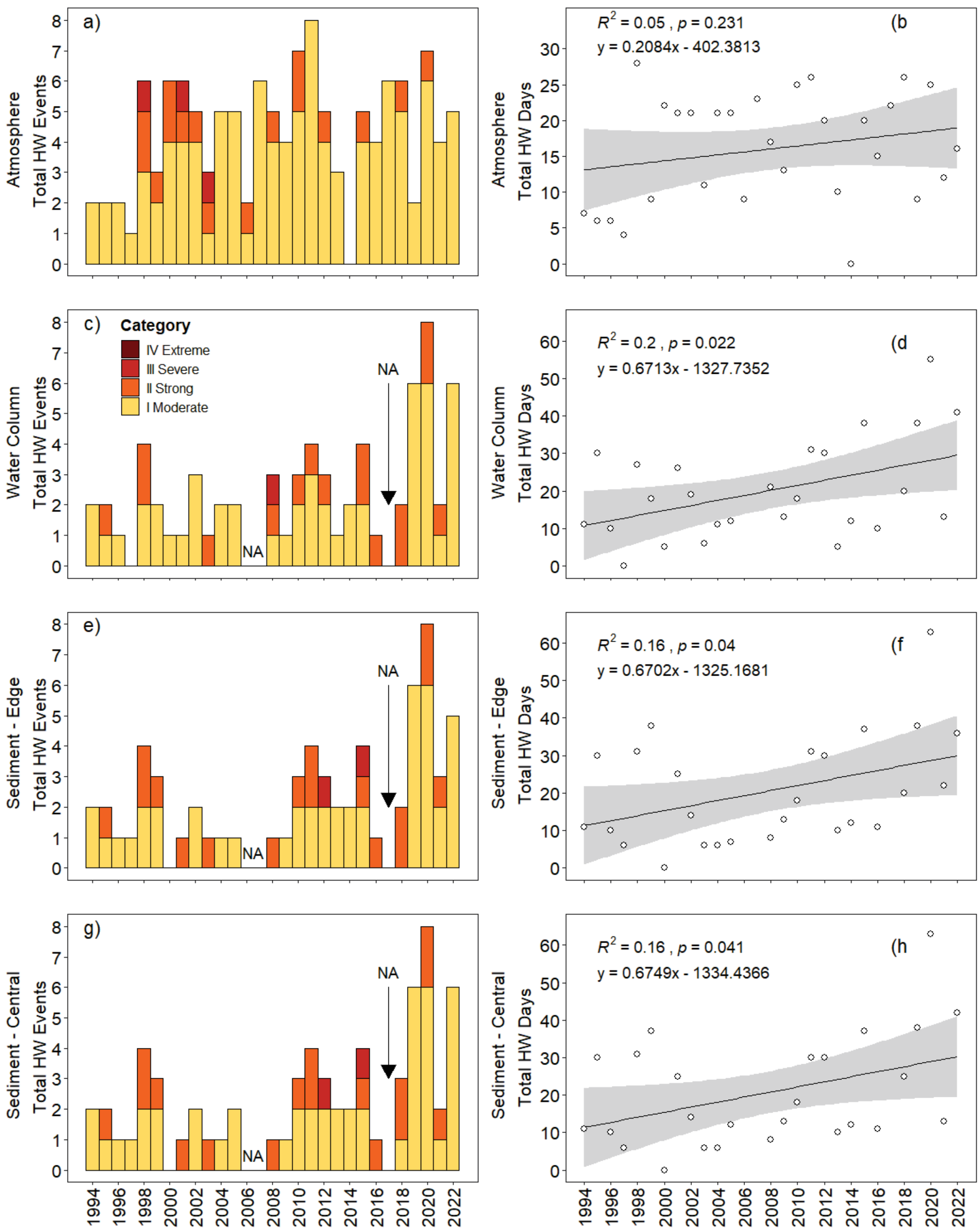

Figure 5. Annual heatwave frequency for the VCR atmosphere (a), the South Bay water column (c), edge (e), and central meadow (g) sediments. Linear regression of the annual total number of heatwave days for the atmosphere (b) water column (d), edge (f), and central meadow sediments (h). NA refers to years when NOAA water temperature and/or water level data was unavailable such that MHW and SHW analyses were not possible.

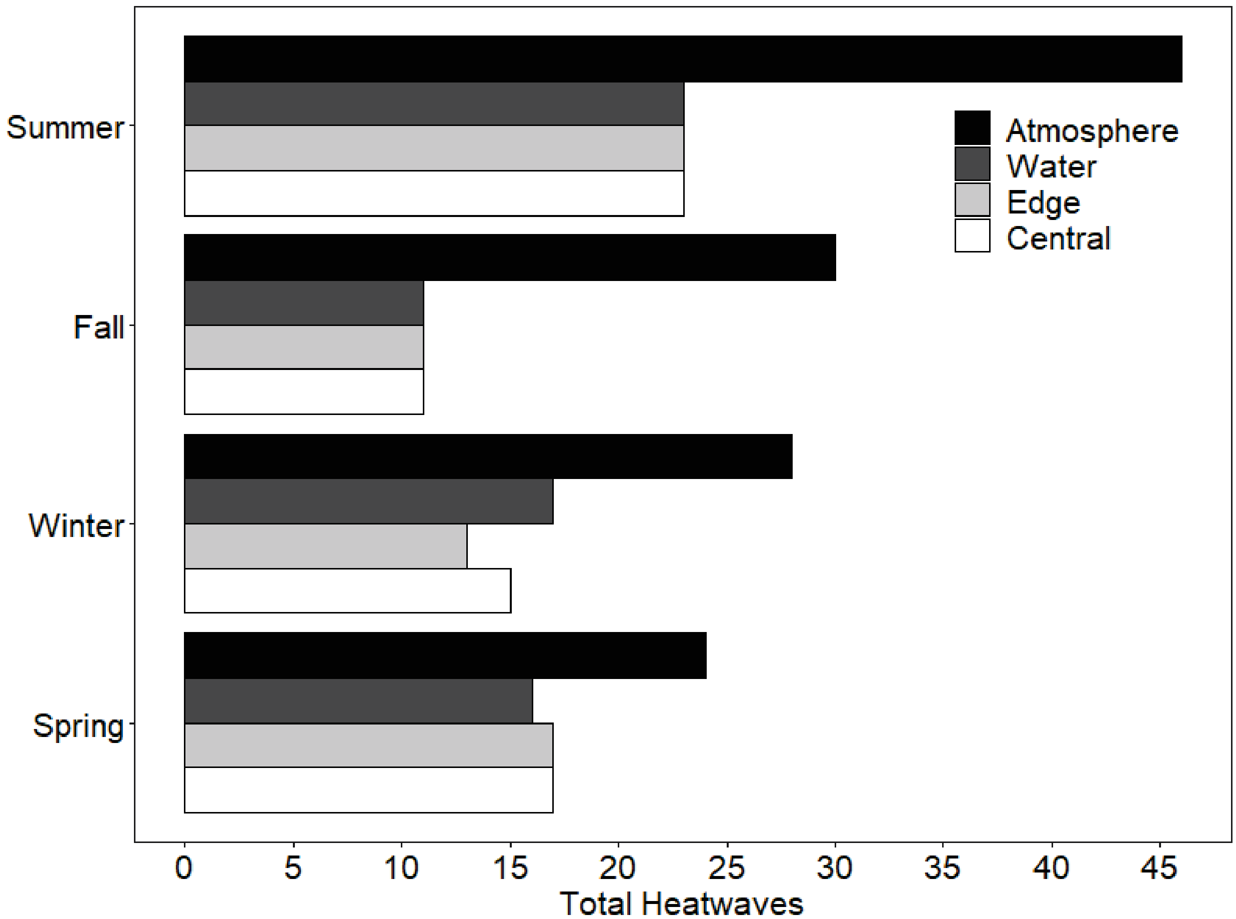

Figure 6. Total number of heatwaves per season for the atmosphere and water column, as well as the central meadow and edge sediments.

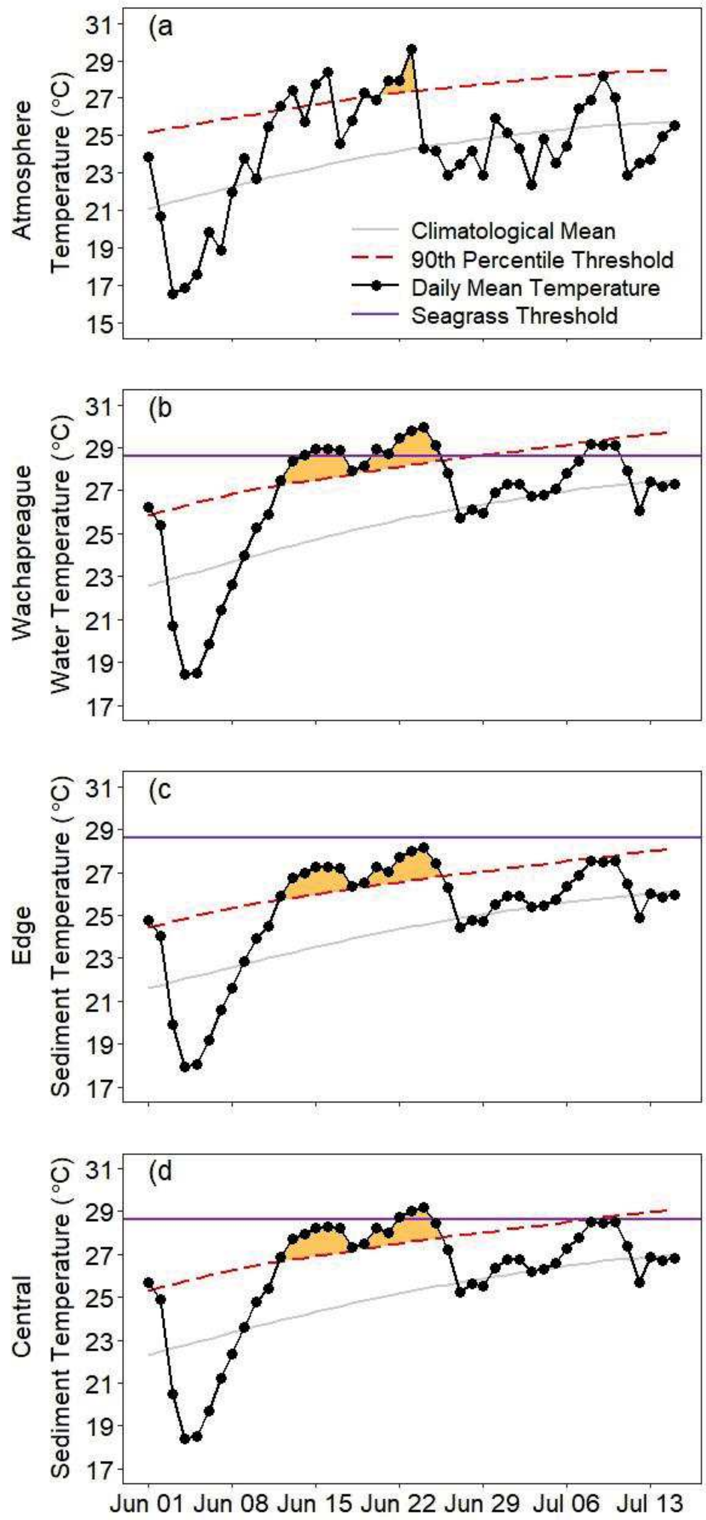

Figure 7. Concurrent heatwaves in the atmosphere (a), water column (b), edge sediments (c), and central meadow (d) sediments. Areas under the curve between the daily mean temperature and 90th percentile represent heatwave conditions. The purple horizontal line in b, c and d represent the 28.6 °C thermal stress threshold for *Z. marina*.